

Optimal Routes to Ultrafast Polarization Reversal in Ferroelectric LiNbO₃

R. Tanner Hardy¹, Conrad Rosenbrock², Gus L. W. Hart², and Jeremy A. Johnson¹

¹ Department of Chemistry and Biochemistry, Brigham Young University, Provo, Utah, USA 84602

² Department of Physics and Astronomy, Brigham Young University, Provo, Utah, USA 84602

Electronic Mail: jjohnson@chem.byu.edu, gus_hart@byu.edu

Abstract:

We use the frozen phonon method to calculate the anharmonic potential energy surface and to model the ultrafast ferroelectric polarization reversal in LiNbO₃ driven by intense pulses of THz light. Before stable switching of the polarization occurs, there exists a region of excitation field-strengths where transient switching can occur, as observed experimentally [Physical Review Letters 118, 197601 (2017)]. By varying the excitation frequency from 4 to 20 THz, our modeling suggests that more efficient, permanent polarization switching can occur by directly exciting the soft mode at 7 THz, compared to nonlinear phononic-induced switching driven by exciting a high frequency mode at 18 THz. We also show that neglecting anharmonic coupling pathways in the modeled experiment can lead to significant differences in the modeled switching field strengths.

A crucial capability to develop high-speed electronic devices is the ability to control atomic structure on picosecond timescales with pulses of light [1,2]. For example, atomic-structure based switches could be developed using ferroelectric materials where structural changes lead to states that are equivalent in energy, but manifest macroscopic polarization that points in opposite directions [3]. These different polarization states can have large enough potential energy barriers as to prevent thermal hopping over the barrier, providing a long-term stable “bit”. Intensive research has been focused on ultrafast light-induced switching of the polarization because theoretical studies have shown picosecond switching times that would enable disruptive advances in the operation speed of non-volatile memory [3-6].

Different experimental routes have been suggested and tested to switch the macroscopic polarization of ferroelectric materials by directly or indirectly driving the zone-center soft mode (the phonon mode with the strongest ties to the polarization). Coherent control methods, also recently termed *nonlinear phononics* [3,4,7-12], involve the simultaneous strong excitation of different atomic motions in the material. In theory, these approaches can lower the potential energy barrier and ease the switching of ferroelectric polarization.

Recently, Mankowsky and co-workers showed, in a somewhat surprising manner, they could *transiently* switch the ferroelectric polarization in LiNbO₃ [10]. With intense pulses of 19 THz light, they resonantly excited the highest frequency A₁ symmetry mode and used a second-harmonic generation (SHG) probe to monitor the sample (see Figs. 1 and 2 in Ref. [10]). The SHG intensity is proportional to the ferroelectric polarization and therefore sensitive to the distance of the Li atoms from the midpoint between two Nb atoms. When LiNbO₃ was excited with high enough fluence, the second harmonic probe intensity was reduced to zero, recovered briefly, then returned to zero intensity, and recovered to the initial intensity in ~1 ps. They interpreted the signal as resulting from the low frequency (soft) A₁ mode being anharmonically driven to such large amplitudes that the Li atoms cross the midpoint between Nb atoms, making it transiently centrosymmetric and stopping SHG. The Li atoms travel some distance on the other side, slightly recovering the SHG with the ferroelectric polarization (and phase of the SHG light) switched.

But surprisingly, the atoms then rebound (crossing the midpoint again) and return to their initial equilibrium positions as the motion is damped on the 1 picosecond timescale. This transient polarization switching was later observed again with an alternative femtosecond stimulated Raman scattering probing scheme [13].

Mankowsky’s experiment attempted to verify a promising computational prediction by Subedi [6], who suggested that the ultrafast reversal of ferroelectric polarization could be accomplished by exciting a high frequency mode that couples anharmonically to the soft A_1 mode. Surprisingly, the experiment showed only temporary polarization reversal, suggesting that the atoms switched and then returned to their original positions.

In this letter, we present first-principles calculations that confirm the possibility of a transient switching of the ferroelectric polarization upon intense THz excitation. We calculated the interatomic potential energy surface (PES), including all of the symmetry-allowed A_1 modes for LiNbO_3 , and then we ran a virtual experiment parallel to the experiments performed in Ref. [10].

To perform these virtual experiments, we fully relaxed the LiNbO_3 structure, we calculated frequencies and eigenvectors of zone-center phonon modes, then we displaced along pairs of phonon modes to reconstruct the anharmonic potential energy surface and extract coupling constants. The structure was relaxed until the force on each atom was less than $4 \times 10^{-4} \text{ eV/\AA}$ ($10^{-5} \text{ Hartree/Bohr}$) and stress on the unit cell was less than 1 kb ($3 \times 10^{-6} \text{ Hartree/Bohr}^3$). Phonon eigenvectors and frequencies were calculated using the DFT-GGA functional as used by Perdew-Burke-Ernzerhof [14], using a plane-wave basis set and Projector Augmented Wave Pseudopotentials (POT-PAW), as implemented in the VASP code [15-19]. By displacing each atom of LiNbO_3 , we calculated the forces on the rest of the atoms to determine the dynamical force matrix. We then used the PHONOPY code [20] to calculate the frequencies and eigenvectors for all the modes (see Fig. 1(a)). We used a $6 \times 6 \times 12$ k-point grid for Brillouin zone integration and a 700 eV cutoff energy for the plane-wave basis expansion.

LiNbO_3 has four phonon modes with A_1 irreducible representations and zone-center frequencies of 7 THz (the “soft” mode), 7.4 THz, 9.0 THz, and 18.3 THz (the 18.3 THz mode was excited in the Refs. [10,13] experiments). Eigenvectors for these modes are shown in Fig. 1(a). We used the frozen phonon method [6,8] to calculate the potential energy surfaces for each pair of the four A_1 zone-center phonon coordinates (six pairwise potential energy surfaces in total). We then fit the calculated potentials to the two-mode potential energy equation (Eq. 1), to obtain the nonlinear coupling coefficients up to 4th order.

$$V(Q_i, Q_j) = \frac{1}{2}\omega_i^2 Q_i^2 + \frac{1}{2}\omega_j^2 Q_j^2 + \sum_{ij} c_{ijk} Q_i Q_j Q_k + \sum_{ij} d_{ijkl} Q_i Q_j Q_k Q_l \quad (\text{Eq. 1})$$

ω_i is the harmonic angular frequency of each vibrational mode, c_{ijk} are the third-order coupling constants, and d_{ijkl} are the fourth order coupling constants. Note that k and l in the sums will only take on values of i and j , because only a pair of modes were used to calculate each surface.

To model the excitation and the resulting polarization dynamics of this system, we treated all four modes as coupled classical underdamped oscillators, experiencing the external driving force due to the electric field of an ultrafast THz pulse. The coupling constants were determined directly from the fits of our six pair-wise potential energy surfaces, and we use experimentally determined linear damping rates for each phonon mode.

We ran our virtual experiment by exciting the system with a ~ 100 fs THz pulse with a central frequency that we vary from ~ 4 to 20 THz. For each central frequency, we then increase the strength of the THz driving field until switching the polarization occurs. Fig. 1(b) shows the modeled time-dependent

ferroelectric polarization for two driving field magnitudes, one below the switching threshold, and one above (showing that the polarization switches direction and stays switched). Figure 1(c) is helpful to consider in understanding the ultrafast atomic motion and polarization switching dynamics. The contour lines in Fig. 1(c) show the potential energy surface determined from displacing the soft A_1 mode at 7 THz and the high frequency A_1 mode at 18 THz. Two local minima are apparent in the PES. The system originates from the minimum on the right, and if the driving field is strong enough to overcome the potential barrier with the correct trajectory, the system will relax to the minimum on the left (corresponding to a reversal of the ferroelectric polarization). The false color map indicates the magnitude of the ferroelectric polarization, with negative (blue) values on the right, and positive (red) values on the left.

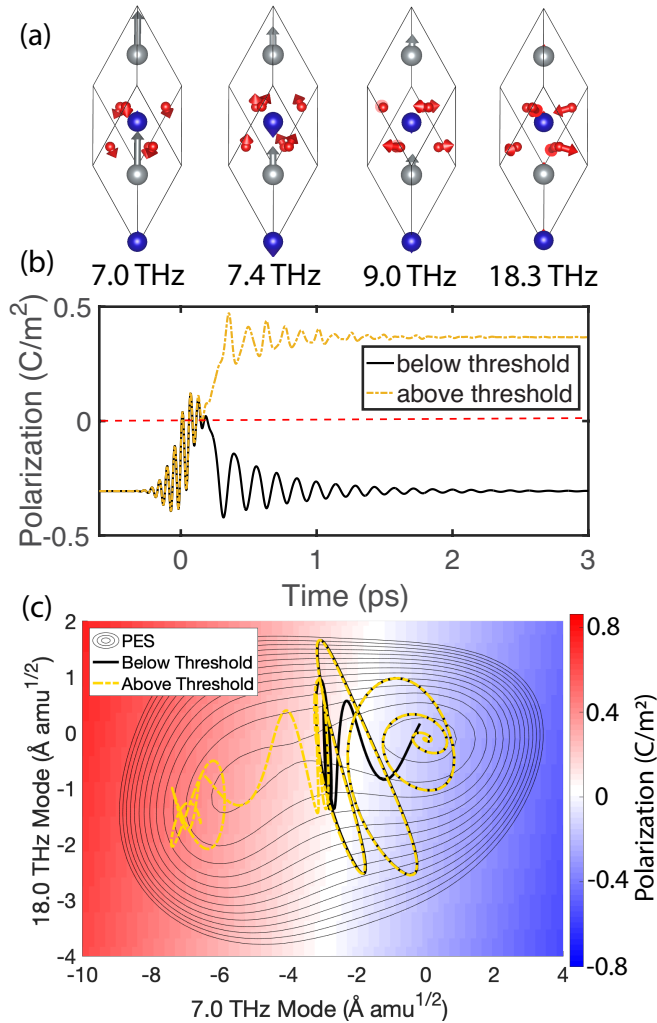


Figure 1. (a) Frequencies and eigenvectors of four A_1 phonon modes in LiNbO_3 . (b) Modeled time-dependent polarization after multi-THz excitation. Black line at lower pump powers below the switching threshold and yellow-orange dash-dotted line above the switching threshold. (c) Contour plot of PES when displacing along 7 and 18 THz A_1 mode coordinates. The black and yellow-orange lines are trajectories for polarization plotted in (b). The false-color scale indicates the polarization for atomic coordinates on the surface.

The orange and black lines show the trajectories for a given THz driving field for the first 0.7 ps, in this case with driving frequency centered at 18 THz. Immediately, coupling between modes during the 100 fs driving pulse results in motion along both phonon coordinates. If the THz pulse is strong enough, the system crosses the potential barrier, permanently relaxing to the minimum with opposite polarization (orange dash-dotted line). If the electric field is not strong enough, the system will always relax back to the starting position (black solid line). Note that even though we plot trajectories only along these two phonon coordinates, the anharmonic coupling calculated from other pairwise potentials between all A_1 phonon coordinates are included in the modeling.

The time-dependent polarization shown in Fig. 1(b) was calculated using the trajectories shown in Fig. 1(c), confirming that a transient switching of ferroelectric polarization is possible; we see that the polarization indicated by the black line crosses the zero point temporarily into the red-shaded region, but then returns to the original static polarization value. A careful inspection of Fig. 1(c) reveals that the point where the magnitude of the ferroelectric polarization goes to zero does not line up exactly with the potential energy barrier, making a transient crossing of the zero-polarization point possible without a permanent switching.

Ref. [10] discussed the possibility that other modes or neighboring ferroelectric domains with opposite polarization could have played a role in the observed transient switching dynamics, which are certainly possibilities. But even in our model that neglects those additional affects, we observe that transient switching of the polarization is possible, and it occurs on identical time scales to what was seen in experiments.

With good agreement to experimental data to validate our approach, we can also use this computational approach to explore other potential methods to accomplish permanent ultrafast polarization switching. For example, we can sweep the central frequency of the pump pulse and determine a relative field strength required to switch the ferroelectric polarization for each pump frequency. Figure 2 shows the relative switching field as a function of central pump frequency. The different blue dashed lines correspond to unique carrier-envelope phases of the pump pulse, and the average switching field is the solid black line.

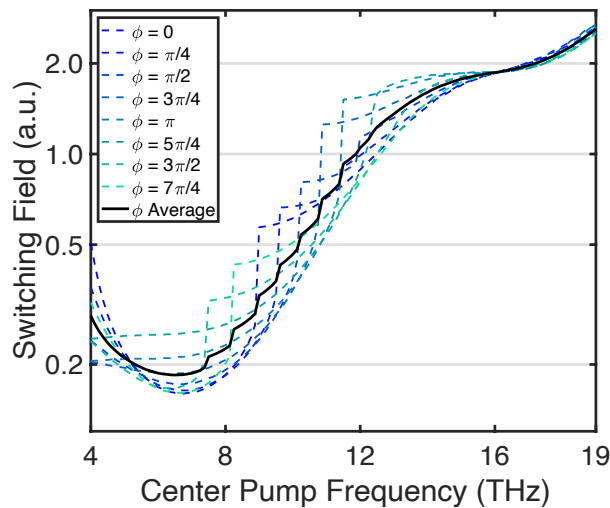


Figure 2. Relative peak electric field required to switch the ferroelectric polarization for specific pump central frequencies. The blue dashed lines indicate specific carrier-envelope phases of the pump pulse, and the solid black line is the average.

We see that the lowest switching field is not close in frequency to the 18 THz mode, but resonant with the lowest frequency 7 THz mode. This mode is the soft mode tied to the ferroelectric polarization, and we see that directly driving the soft mode is predicted to be the most efficient route to polarization switching, with a $\sim 10\times$ lower switching field than required when utilizing anharmonic coupling of the high frequency mode. This suggests that directly pumping the soft mode should be the most efficient route to ferroelectric polarization reversal in LiNbO_3 .

We can also compare our four-mode model with a simpler model similar to previous work in Ref. [6] that only included two modes in the calculations: the high-frequency 18 THz mode and the 7 THz soft mode. We compute the average switching field as a function of frequency for both models. Figure 3 shows the percent difference in switching field comparing the two models for LiNbO_3 . A value larger than zero indicates that the two-mode model predicts a higher switching field than the four-mode model, and a value less than zero indicates the four-mode model predicts a lower switching field. We see that at high frequencies, the two-mode model underestimates the switching field. This difference arises from the fact that the other two A_1 phonon modes at 7.4 THz and 9 THz also couple to the high frequency phonon, and some energy deposited in the high frequency mode transfers to these two modes instead of the soft mode motion that corresponds to polarization switching.

On the other hand, at lower frequencies from ~ 5 to 10 THz, the four-mode model predicts a lower switching field than the two-mode model. This lower predicted field arises due to the moderate bandwidth of the pump pulse. With the frequency centered below 8 THz, the THz pulse resonantly drives not only soft mode, but also the other two low-frequency modes. We directly put energy into the soft mode with the driving field, but then additional energy can flow to the soft mode via coupling with the other two resonantly excited modes. Both of these cases (excitation at higher and lower frequencies) indicate that the anharmonic interactions to other modes with symmetry-allowed couplings should not be neglected when trying to predict ultrafast dynamics.

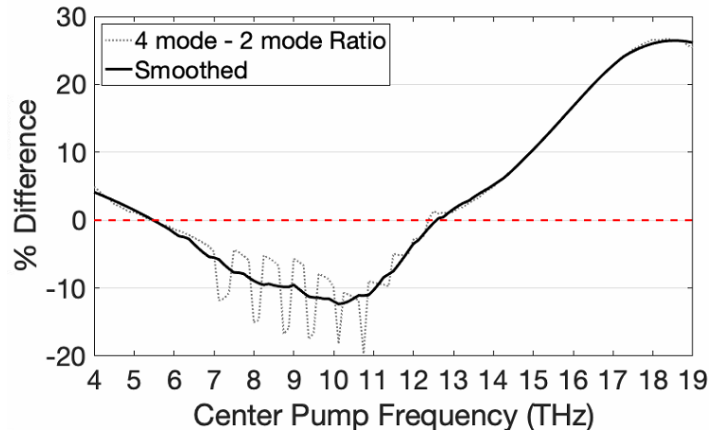


Figure 3. Ratio of peak switching field of the four-mode model compared to the two-mode model, showing the two-mode model does not accurately capture the switching dynamics at low and high frequencies.

Finally, with our more complete four-mode model that shows good agreement to experimental data, we can also investigate methods to tailor the excitation pulses to reverse the ferroelectric polarization more efficiently. For example, we hypothesize that a linearly chirped pump pulse with lower frequencies within the pump bandwidth arriving later could more efficiently drive the motion as the PES softens going across the potential barrier between polarization states.

In conclusion, we have used the frozen phonon method to model ferroelectric polarization switching in LiNbO₃. We find that under certain conditions, we can reproduce with nearly identical temporal dynamics the transient switching of polarization observed by Mankowsky et al. [10]. We show that neglecting symmetry allowed anharmonic couplings to other modes in the modeling can lead to significant differences in predicted switching field strengths. Furthermore, we vary the excitation frequency to show that significantly lower switching fields are predicted to occur when resonantly driving the soft mode, rather than driving a higher frequency mode that couples to the soft mode. The idea that directly exciting the soft mode to achieve polarization switching should warrant more investigation. Particularly due to reports of using meta-material layers or antennas to locally enhance THz electric fields [21-28]; these local enhancement methods work better with lower frequencies due to larger feature sizes and easier fabrication.

References

- [1] Y. Xu, in *Ferroelectric Materials and their Applications*, edited by Y. Xu (Elsevier, Amsterdam, 1991), pp. 1.
- [2] L. W. Martin and A. M. Rappe. Thin-film ferroelectric materials and their applications. *Nature Reviews Materials* **2**, 16087 (2016). <https://doi.org/10.1038/natrevmats.2016.87>
- [3] T. Qi, Y.-H. Shin, K.-L. Yeh, K. A. Nelson, and A. M. Rappe. Collective Coherent Control: Synchronization of Polarization in Ferroelectric PbTiO₃ by Shaped THz Fields. *Physical Review Letters* **102**, 247603 (2009). <http://link.aps.org/doi/10.1103/PhysRevLett.102.247603>
- [4] X. Li, T. Qiu, J. Zhang, E. Baldini, J. Lu, A. M. Rappe, and K. A. Nelson. Terahertz field-induced ferroelectricity in quantum paraelectric SrTiO₃. *Science* **364**, 1079 (2019). <http://science.sciencemag.org/content/364/6445/1079.abstract>
- [5] T. F. Nova, A. S. Disa, M. Fechner, and A. Cavalleri. Metastable ferroelectricity in optically strained SrTiO₃. *Science* **364**, 1075 (2019). <http://science.sciencemag.org/content/364/6445/1075.abstract>
- [6] A. Subedi. Proposal for ultrafast switching of ferroelectrics using midinfrared pulses. *Physical Review B* **92**, 214303 (2015). <https://link.aps.org/doi/10.1103/PhysRevB.92.214303>
- [7] B. S. Dasturp, J. R. Hall, and J. A. Johnson. Experimental determination of the interatomic potential in LiNbO₃ via ultrafast lattice control. *Applied Physics Letters* **110**, 162901 (2017). <http://dx.doi.org/10.1063/1.4980112>
- [8] D. M. Juraschek, M. Fechner, and N. A. Spaldin. Ultrafast Structure Switching through Nonlinear Phononics. *Physical Review Letters* **118**, 054101 (2017). <https://link.aps.org/doi/10.1103/PhysRevLett.118.054101>
- [9] D. M. Juraschek and S. F. Maehrlein. Sum-frequency ionic Raman scattering. *Physical Review B* **97**, 174302 (2018). <https://link.aps.org/doi/10.1103/PhysRevB.97.174302>
- [10] R. Mankowsky, A. von Hoegen, M. Först, and A. Cavalleri. Ultrafast Reversal of the Ferroelectric Polarization. *Physical Review Letters* **118**, 197601 (2017). <https://link.aps.org/doi/10.1103/PhysRevLett.118.197601>
- [11] A. Subedi, A. Cavalleri, and A. Georges. Theory of nonlinear phononics for coherent light control of solids. *Physical Review B* **89**, 220301 (2014). <https://link.aps.org/doi/10.1103/PhysRevB.89.220301>
- [12] A. von Hoegen, R. Mankowsky, M. Fechner, M. Först, and A. Cavalleri. Probing the interatomic potential of solids with strong-field nonlinear phononics. *Nature* **555**, 79 (2018). <http://dx.doi.org/10.1038/nature25484>

- [13] M. Henstridge, M. Först, E. Rowe, M. Fechner, and A. Cavalleri. Nonlocal nonlinear phononics. *Nature Physics* **18**, 457 (2022). <https://doi.org/10.1038/s41567-022-01512-3>
- [14] J. P. Perdew, K. Burke, and M. Ernzerhof. Generalized Gradient Approximation Made Simple. *Physical Review Letters* **77**, 3865 (1996). <https://link.aps.org/doi/10.1103/PhysRevLett.77.3865>
- [15] G. Kresse and J. Furthmüller. Efficiency of ab-initio total energy calculations for metals and semiconductors using a plane-wave basis set. *Computational Materials Science* **6**, 15 (1996). <https://www.sciencedirect.com/science/article/pii/0927025696000080>
- [16] G. Kresse and J. Furthmüller. Efficient iterative schemes for ab initio total-energy calculations using a plane-wave basis set. *Physical Review B* **54**, 11169 (1996). <https://link.aps.org/doi/10.1103/PhysRevB.54.11169>
- [17] G. Kresse and J. Hafner. Ab initio molecular dynamics for liquid metals. *Physical Review B* **47**, 558 (1993). <https://link.aps.org/doi/10.1103/PhysRevB.47.558>
- [18] G. Kresse and J. Hafner. Ab initio molecular-dynamics simulation of the liquid-metal--amorphous-semiconductor transition in germanium. *Physical Review B* **49**, 14251 (1994). <https://link.aps.org/doi/10.1103/PhysRevB.49.14251>
- [19] G. Kresse and D. Joubert. From ultrasoft pseudopotentials to the projector augmented-wave method. *Physical Review B* **59**, 1758 (1999). <https://link.aps.org/doi/10.1103/PhysRevB.59.1758>
- [20] A. Togo and I. Tanaka. First principles phonon calculations in materials science. *Scripta Materialia* **108**, 1 (2015). <https://www.sciencedirect.com/science/article/pii/S1359646215003127>
- [21] T. L. Cocker, D. Peller, P. Yu, J. Repp, and R. Huber. Tracking the ultrafast motion of a single molecule by femtosecond orbital imaging. *Nature* **539**, 263 (2016). <http://dx.doi.org/10.1038/nature19816>
- [22] K. Fan, H. Y. Hwang, M. Liu, A. C. Strikwerda, A. Sternbach, J. Zhang, X. Zhao, X. Zhang, K. A. Nelson, and R. D. Averitt. Nonlinear Terahertz Metamaterials via Field-Enhanced Carrier Dynamics in GaAs. *Physical Review Letters* **110**, 217404 (2013). <https://link.aps.org/doi/10.1103/PhysRevLett.110.217404>
- [23] C. Feuillet-Palma, Y. Todorov, A. Vasanelli, and C. Sirtori. Strong near field enhancement in THz nano-antenna arrays. *Scientific Reports* **3**, 1361 (2013). <http://dx.doi.org/10.1038/srep01361>
- [24] C. Lange, T. Maag, M. Hohenleutner, S. Baierl, O. Schubert, E. R. J. Edwards, D. Bougeard, G. Woltersdorf, and R. Huber. Extremely Nonperturbative Nonlinearities in GaAs Driven by Atomically Strong Terahertz Fields in Gold Metamaterials. *Physical Review Letters* **113**, 227401 (2014). <https://link.aps.org/doi/10.1103/PhysRevLett.113.227401>
- [25] M. Liu, H. Y. Hwang, H. Tao, A. C. Strikwerda, K. Fan, G. R. Keiser, A. J. Sternbach, K. G. West, S. Kittiwatanakul, J. Lu, S. A. Wolf, F. G. Omenetto, X. Zhang, K. A. Nelson, and R. D. Averitt. Terahertz-field-induced insulator-to-metal transition in vanadium dioxide metamaterial. *Nature* **487**, 345 (2012). <http://dx.doi.org/10.1038/nature11231>
- [26] A. Novitsky, A. M. Ivinskaya, M. Zalkovskij, R. Malureanu, P. Uhd Jepsen, and A. V. Lavrinenko. Non-resonant terahertz field enhancement in periodically arranged nanoslits. *Journal of Applied Physics* **112**, 074318 (2012). <https://doi.org/10.1063/1.4757024>
- [27] M. A. Seo, H. R. Park, S. M. Koo, D. J. Park, J. H. Kang, O. K. Suwal, S. S. Choi, P. C. M. Planken, G. S. Park, N. K. Park, Q. H. Park, and D. S. Kim. Terahertz field enhancement by a metallic nano slit operating beyond the skin-depth limit. *Nature Photonics* **3**, 152 (2009). <http://dx.doi.org/10.1038/nphoton.2009.22>
- [28] C. A. Werley, K. Fan, A. C. Strikwerda, S. M. Teo, X. Zhang, R. D. Averitt, and K. A. Nelson. Time-resolved imaging of near-fields in THz antennas and direct quantitative measurement of field

enhancements. Opt. Express **20**, 8551 (2012). <http://www.opticsexpress.org/abstract.cfm?URI=oe-20-8-8551>